

## Spectral Filtering in Neutron Interferometry

S. A. Werner, R. Clothier,<sup>(a)</sup> and H. Kaiser*Physics Department and Research Reactor Facility, University of Missouri-Columbia, Columbia, Missouri 65211*

H. Rauch and H. Wölwitsch

*Atominstitut der Österreichischen Universitäten, A-1020 Vienna, Austria*

(Received 6 May 1991)

We have demonstrated experimentally that the contrast lost, due to placing slabs of a material having a neutron optical potential in one leg of a neutron interferometer, can be restored by spectral filtering of the beams leaving the interferometer immediately before detection. The non-Gaussian spectral distribution of the neutrons traversing the interferometer in our experiment leads to an unexpected phase reversal of the interferograms.

PACS numbers: 42.50.-p, 03.65.Bz

The evolution of the wave function  $\psi(\mathbf{r}, t)$  of a freely propagating neutron in a beam having a Gaussian spectral distribution is described (in part) by the well-known expression for the time-dependent longitudinal spatial length [1]:

$$\sigma_x^2(t) = \sigma_x^2(0) + [\hbar t / 2m\sigma_x(0)]^2, \quad (1)$$

where  $m$  is the neutron mass. The minimum length  $\sigma_x(0)$  is related to the spectral width  $\sigma_k$  of the linear superposition of plane waves  $a(k)e^{i(kx - \omega t)}$  by the uncertainty relation

$$\sigma_x(0)\sigma_k \geq \frac{1}{2}. \quad (2)$$

For a spectral distribution which is precisely Gaussian, the equality holds. If the wave packet traversing one leg of a neutron interferometer is delayed (displaced in space), say, by passage through a slab of material having an optical potential  $V_{op}$ , relative to the wave packet traversing the other leg of the interferometer, they will no longer spatially overlap in the region of recombination, and the interference contrast will disappear. For this to occur, the relative displacement  $\Delta l$  of the two wave packets need only be a small multiple of the minimum spatial width  $\sigma_x(0)$  and not of the much larger width  $\sigma_x(t)$  [2]. This fact was demonstrated in an experiment by Kaiser, Werner, and George [3] designed to measure the longitudinal coherence length of a neutron beam, and explained in a straightforward way by Klein, Opat, and Hamilton [4]. A detailed treatment of coherence phenomena in neutron interferometry dealing with these matters is given by Petrascheck [5].

In an actual neutron interferometry experiment there is no *a priori* reason to believe that the spectral distribution  $g(k) = |a(k)|^2$  is precisely Gaussian, since it depends in detail on the mosaic spread of the monochromator, the collimators before and after the monochromator, and the Bragg angles of the interferometer and the monochromator. We show here that the non-Gaussian nature of a real neutron beam gives rise to some interesting and (initially) unexpected effects in neutron interferometry. Further-

more, we have demonstrated experimentally, for the first time, that the interference contrast lost due to relative spatial displacement of the waves traversing the two legs of the interferometer can be partially restored by spectral filtering of the beams immediately before detection.

The experiment was carried out using the skew-symmetric interferometer at beam port C at the University of Missouri Research Reactor. A schematic diagram of the setup is shown in Fig. 1. Neutrons of mean wavelength  $\bar{\lambda} = 2.349 \text{ \AA}$  from a pyrolytic graphite (002) monochromator ( $2\theta_M = 41^\circ$ ) are incident upon the perfect silicon crystal interferometer. The (220) lattice planes are used in the interferometer ( $2\theta_B = 75.4^\circ$ ). The beam on path II passes through a series of highly polished Bi metal slabs of total thickness  $D$ . Bismuth has negligible neutron absorption, and a positive neutron-nuclear scattering

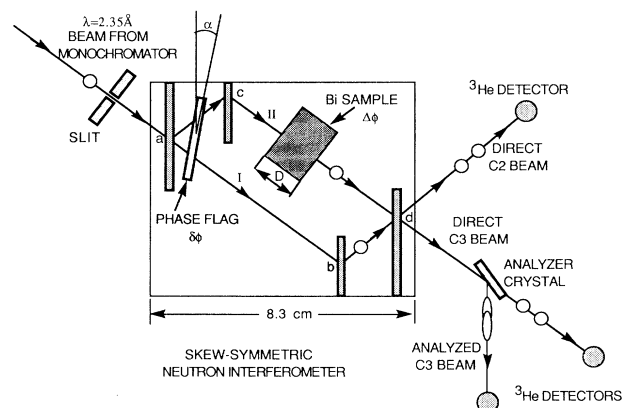


FIG. 1. Schematic diagram of a perfect Si crystal skew-symmetric interferometer. The beam from the monochromator, of nominal wavelength  $\lambda = 2.35 \text{ \AA}$ , passes through a slit  $8 \text{ mm} \times 6 \text{ mm}$  immediately in front of the interferometer. The beam on path II passes through a series of bismuth slabs, which spatially delay the neutron due to the positive optical potential of Bi. The C3 beam is detected after reflecting from a Si analyzer crystal. The interference contrast is measured by rotating the aluminum phase flag in steps  $\alpha$  about a vertical axis.

length  $b=8.533$  fm. We refer to these Bi slabs as the sample. The neutron optical potential of a bismuth metal sample of atom density  $N$  is [6]

$$V_{\text{op}}=2\pi\hbar^2Nb/m=6.24\times 10^{-5}\text{ meV}, \quad (3)$$

which is small compared to the neutron's kinetic energy,  $E=14.7$  meV. Thus, due to passage through the Bi sample, the neutron wave function on path II is displaced longitudinally by a small amount

$$\Delta l = \frac{1}{2} DV_{\text{op}}/E, \quad (4)$$

and experiences a phase shift

$$\Delta\phi = -\lambda NbD. \quad (5)$$

The relative longitudinal displacement of the two wave functions indicated schematically in Fig. 1 is greatly exaggerated. For 1 cm of Bi,  $\Delta l=212$  Å and  $\Delta\phi=-565$  rad. The wave functions  $\psi_I(\mathbf{r},t)$  and  $\psi_{II}(\mathbf{r},t)$  traversing the paths I and II can be viewed as wave packets which recombine in the fourth Si crystal slab near point  $d$ . The two interfering beams leaving the interferometer, labeled C2 and C3, are composed of linear combinations of  $\psi_I$  and  $\psi_{II}$ . We place a Bragg reflecting crystal in the C3 beam to select out of the spectral distribution  $g(k)$  a window  $w(k)$  of Fourier components  $k$ . Because of the narrower spectral width of the analyzed C3 beam, quantum mechanics suggests that the corresponding wave packets are spatially lengthened, and may again substantially overlap and interfere, even though the two wave packets traversing paths I and II were by no means spatially coincident in the final recombining Si crystal of the interferometer. The signature of this effect is the observed recovery of lost contrast of the interferogram, which we now discuss.

Neutrons leaving the interferometer are swapped back and forth between the C2 and C3 beams in an oscillatory, neutron-current-conserving manner as a function of the phase difference  $\Delta\Phi=\Phi_{II}-\Phi_I$  for waves traveling on path II relative to path I, such that

$$I_2 = C + B \int_{-\infty}^{\infty} g(k) \cos(\Delta\Phi) dk, \quad (6)$$

$$I_3 = A - B \int_{-\infty}^{\infty} g(k) \cos(\Delta\Phi) dk, \quad (7)$$

where  $A$ ,  $B$ , and  $C$  are constants characterizing the interferometer and the incident beam intensity. For a perfect interferometer  $A=B$  and  $C\approx 2.7A$ , as discussed elsewhere [7]. For the conditions of the experiment described here  $B/A\approx 0.5$ , so that the maximum contrast was about 50%. The fringe visibility, or contrast,  $(I_{\text{max}}-I_{\text{min}})/(I_{\text{max}}+I_{\text{min}})$ , is obtained from the mutual coherence function

$$\Gamma(D, \alpha) = \langle \psi_I^*(0) \psi_{II}(\Delta l) \rangle = \frac{1}{\sqrt{2\pi}} \int_{-\infty}^{\infty} g(k) (\cos\Delta\Phi) dk, \quad (8)$$

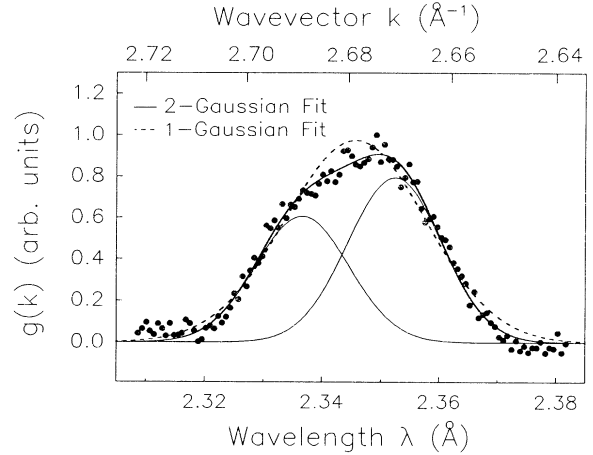


FIG. 2. Measured spectral distribution  $g(k)$  in the C3 beam. The parameters for the one-Gaussian fit are  $a=0.974$ ,  $\lambda_0=2.3456$  Å,  $\sigma_\lambda=0.0120$  Å. The parameters for the two-Gaussian fit are  $a_1=0.606$ ,  $\lambda_{11}=2.3366$  Å,  $\sigma_{\lambda_1}=0.00798$  Å, and  $a_2=0.793$ ,  $\lambda_{21}=2.3524$  Å,  $\sigma_{\lambda_2}=0.00800$  Å.

where  $\Delta\Phi$  is the sum of  $\Delta\phi(D)$  given by Eq. (5) and the phase shift  $\delta\phi(\alpha)$  due to the phase flag. We explicitly note the dependence of  $\Gamma$  on the thickness  $D$  of the Bi slabs and the angle  $\alpha$  of the phase flag, since these are the parameters which are varied in our experiment. The expressions (6), (7), and (8) can be obtained from general arguments [8]. Since the mutual coherence function depends only upon  $|a(k)|^2$ , it is not possible to obtain information on the relative phasing of the Fourier components making up the wave packets. For example, an incoherent superposition of plane waves gives the same result.

We show in Fig. 2 the results of a measurement of the spectral distribution  $g(k)$  of the neutrons in the C3 beam, obtained from a rocking curve of a nearly perfect Si(111) crystal in the antiparallel (nondispersive) configuration. The spectral acceptance width of this analyzer crystal is  $7\times 10^{-4}$  Å, corresponding to an effective mosaic width of  $0.02^\circ$ . A single Gaussian with the parameters given in the figure caption is a reasonable fit to the data. With a given thickness of Bi in leg II of the interferometer, we measure the contrast by rotating the phase flag in steps  $\alpha$ , and compare the contrast of this interferogram with that obtained with the Bi sample removed. We call the ratio the relative contrast. The results are shown in Fig. 3(a). The contrast falls off with Bi thickness  $D$  as expected. However, there is a long tail which we initially found to be perplexing. For a Gaussian  $g(k)$ , Eq. (8) suggests that the relative contrast should be a Gaussian function of  $D$ , namely, the magnitude of the oscillations of the mutual coherence function [9]

$$\frac{\Gamma(D, \alpha)}{\Gamma(0, 0)} = \exp\left\{-\frac{1}{2}(NbD\sigma_\lambda)^2\right\} \cos(-NbD\bar{\lambda} + \delta\phi), \quad (9)$$

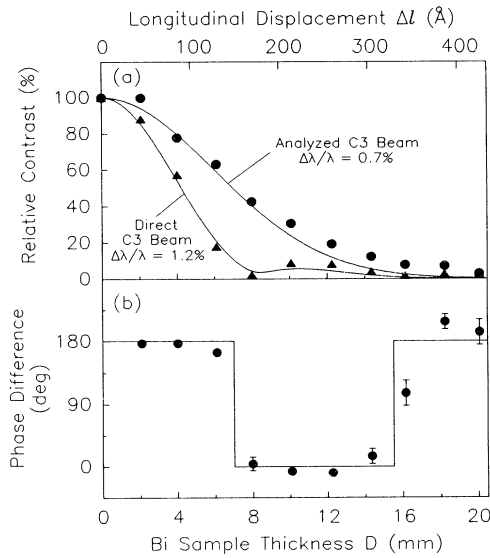


FIG. 3. (a) Plot of the relative contrast in the direct C3 beam and also in the analyzed C3 beam as a function of the bismuth slab thickness,  $D$ . The widths of the spectral distributions  $g(k)$  of the direct C3 beam and the analyzed C3 beam are  $\Delta\lambda/\lambda=1.2\%$  and  $\Delta\lambda/\lambda=0.7\%$ , respectively. The solid lines are the result of calculating the mutual coherence function based upon the measured spectral distribution (Fig. 2) and the measured Gaussian mosaic width of the pressed Si analyzer crystal. (b) A plot of the phase difference between the direct C2 beam interferogram and the analyzed C3 beam interferogram.

where the Gaussian width  $\sigma_\lambda$  of the wavelength spectrum is given by  $\sigma_\lambda=2\pi\sigma_k/k^2$ , and  $\bar{\lambda}$  is the mean wavelength. This formula becomes slightly more complicated if beam attenuation is included and the sample is not oriented perpendicular to the beam [10]. One might suspect that the long tail on the contrast curve is due to an undetected sharp component of  $g(k)$ . This turns out not to be the case. The correct explanation comes from the fact that small deviations from a Gaussian  $g(k)$  lead to important, unanticipated, and measurable effects. This can be seen by supposing  $g(k)$  can be modeled by two closely spaced Gaussian peaks, as shown in Fig. 2, namely,

$$g(k) = a_1 \exp\left\{-(k-k_1)^2/2\sigma_1^2\right\} + a_2 \exp\left\{-(k-k_2)^2/2\sigma_2^2\right\}. \quad (10)$$

For the simplest case of two Gaussians with equal heights and widths, it is easy to show that the mutual coherence function is

$$\frac{\Gamma(D,\alpha)}{\Gamma(0,0)} = \cos(NbD\Delta\lambda) \exp\left\{-\frac{1}{2}(NbD\sigma_\lambda)^2\right\} \times \cos(-NbD\bar{\lambda} + \delta\phi), \quad (11)$$

where  $\Delta\lambda=(\lambda_2-\lambda_1)/2$  and  $\bar{\lambda}=(\lambda_1+\lambda_2)/2$ . Thus, when  $NbD\Delta\lambda \rightarrow \pi/2$ , the contrast goes to zero, and then rises to a secondary maximum before falling off into the noise. The solid curves in Fig. 3(a) are the result of evaluating

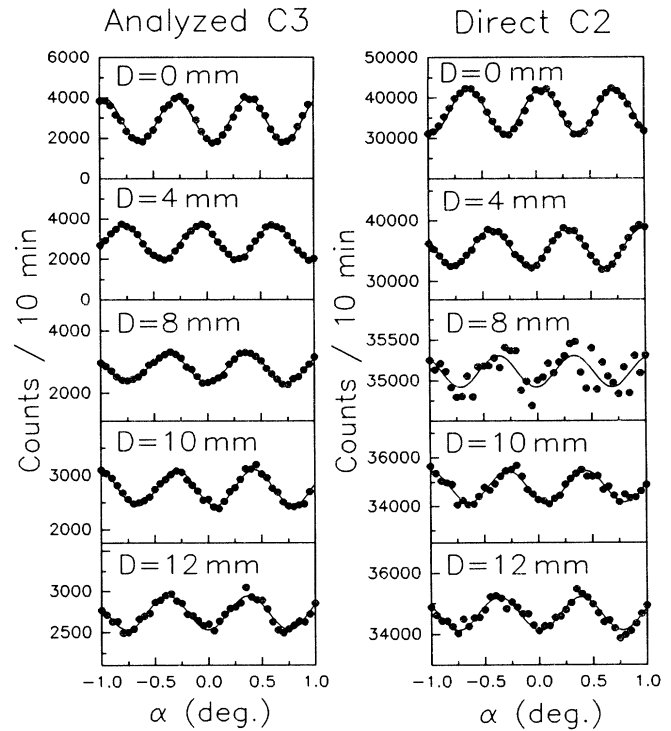


FIG. 4. Interferograms obtained by rotating the phase flag through small angles  $\alpha$ , for the direct C2 beam and the analyzed C3 beam for various Bi slab thicknesses,  $D$ . Note that these interferograms are  $180^\circ$  out of phase for  $D < 8$  mm, but are in phase for  $D = 10$  and 12 mm.

$\Gamma(D,\alpha)$  using the two-Gaussian fit to the measured spectrum  $g(k)$  shown in Fig. 2.

We turn now to a discussion of the interferograms obtained in the analyzed C3 beam, in which a pressed Si(111) crystal with a mosaic width  $\eta(\text{FWHM})=0.47^\circ$  was used as the analyzer in the antiparallel configuration. The spectral width of this analyzed C3 beam was calculated to be  $\Delta\lambda/\lambda=0.7\%$ . Figure 4 displays a representative series of analyzed C3 beam interferograms in the left-hand panels in comparison to the direct C2 beam interferograms shown in the right-hand panels. Note the change of the scale of the ordinate for increasing Bi slab thicknesses. With the analyzer crystal in place, we did not measure the direct C3 interferograms, but we know from the data discussed above that the magnitude of the interference oscillation in the direct C3 beam is the same as the magnitude of the oscillations of the direct C2 beam; they are always  $180^\circ$  out of phase. The relative contrast in the analyzed C3 beam persists to considerably larger Bi thicknesses. For example, when the relative contrast in the direct beams has fallen to zero near  $D=8$  mm [Fig. 3(a)], the relative contrast of the analyzed C3 beam interferogram is still about 40%. The predicted recovery of lost contrast by this wavelength filtering just before detection is evident.

In a manner anticipated from the relative phasing of the direct C2 and C3 interferograms, the relative phases of the analyzed C3 interferograms and the direct C2 interferograms are also  $180^\circ$  for Bi sample thicknesses  $D=0$  up to  $\approx 8$  mm. However, in the region  $D \approx 8$  to  $\approx 16$  mm, the phase of the analyzed C3 interferogram relative to the direct C2 interferogram is  $0^\circ$ . For  $D > 16$  mm, these two interferograms are again  $180^\circ$  out of phase. A summary of these relative phase data is shown in Fig. 3(b). Initially, this switching of the relative phases of these interferograms was surprising. The origin of this effect comes from the small deviations of the direct C2 and C3 spectral distributions  $g(k)$  from a perfect Gaussian, and can be understood from the expression for the mutual coherence function given in Eq. (11). When the value of  $NbD\Delta\lambda$  passes through  $\pi/2$ ,  $3\pi/2$ , etc., the phase of the direct beam interferograms given by Eqs. (6) and (7) abruptly changes by  $180^\circ$  due to the factor  $\cos(NbD\Delta\lambda)$  in  $\Gamma(D, \alpha)$ . For the analyzed C3 beam the spectral distribution is accurately represented by a single (narrower) Gaussian [i.e.,  $\Delta\lambda=0$  in Eq. (11)]. Thus, a comparison of the relative phase of the analyzed C3 beam interferogram with the direct C2 beam interferogram provides a subtle, but direct signature of the non-Gaussian nature of the spectral distribution of the beams traversing the interferometer.

Although our method of modeling small deviations of  $g(k)$  from a Gaussian by two closely spaced Gaussians is *ad hoc*, we believe that the essential physics of the phase switching and contrast modulations shown in Fig. 3 is captured by this model. These experiments represent the first observation of this effect, and the first observation of recovering contrast by spectral filtering immediately before detection in matter wave interferometry.

This work was supported by the Physics Division of the NSF (Grant No. PHY-8813253), the U.S.-Austria program at NSF (Grant No. INT-8712122), and Fonds zur Förderung der wissenschaftlichen Forschung (Project No. S4201) in Austria.

(a)Present address: Physics Department, Bethany College, Bethany, WV 26032.

- [1] A. Messiah, *Quantum Mechanics* (Elsevier/North-Holland, New York, 1961), Vol. 1, p. 222; see also L. Cohen, *Found. Phys.* **20**, 1455 (1990).
- [2] For the experimental conditions described in this paper,  $\sigma_k = 0.0105 \text{ \AA}^{-1}$ , so that  $\sigma_x(0)$  is approximately  $48 \text{ \AA}$ , i.e., the longitudinal length is  $\Delta x = 2\sqrt{2 \ln 2} (48 \text{ \AA}) = 110 \text{ \AA}$ . The neutron time of flight across the interferometer is about  $47 \mu\text{sec}$ ; thus,  $\sigma_x(t = 47 \mu\text{sec}) = 3 \times 10^6 \text{ \AA}$ .
- [3] H. Kaiser, S. A. Werner, and E. A. George, *Phys. Rev. Lett.* **50**, 560 (1983).
- [4] A. G. Klein, G. I. Opat, and W. A. Hamilton, *Phys. Rev. Lett.* **50**, 563 (1983).
- [5] D. Petrascheck, *Phys. Rev. B* **35**, 6549 (1987).
- [6] V. Sears, *Neutron Optics* (Oxford Univ. Press, New York, 1989), Chap. 2.
- [7] S. A. Werner and A. G. Klein, in *Neutron Scattering*, edited by K. Sköld and D. L. Price, *Methods of Experimental Physics* Vol. 23A (Academic, New York, 1986), Chap. 2, pp. 303–308.
- [8] See, for example, H. J. Bernstein and F. E. Low, *Phys. Rev. Lett.* **59**, 951 (1987).
- [9] H. Rauch and M. Suda, *Phys. Status Solidi (a)* **25**, 495 (1974).
- [10] H. Rauch, E. Seidl, D. Tuppinger, D. Petrascheck, and R. Scherm, *Z. Phys. B* **69**, 313 (1987); see also R. Clothier, Ph.D. thesis, University of Missouri-Columbia, 1991 (unpublished).